FUN WITH FRACTALS

John Cobb, Eric Astor, Eugene Astrakan, Christine Boone,
Dhruva Chandramohan, Alexandra Konings, Stephanie Mok,
Scott Weingart, Benjamin Wieder, Matthew Zegarek

Advisor: Dr. Paul Victor Quinn Sr.
Assistant: Karl Strohmaier

ABSTRACT

Fractals are mathematical structures that have some degree of self-similarity and scale independence. As well as being intrinsically interesting from a purely theoretical standpoint, fractals are useful in many arenas. This paper explores the use of fractals in diverse fields including the more theoretical Sierpinski fractals, Mandelbrot, and Julia sets and the more practical areas of modeling natural and physical systems. Ultimately, this knowledge of fractals is used to explore a model of a ball bouncing on an oscillating plate from a different point of view

INTRODUCTION

Fractals and chaos theory are some of the most popular and burgeoning fields of contemporary mathematics. Fractals were first discussed in the late 19th century in the form of nested two-dimensional drawings created in order to debunk the ideas of limits in calculus. These designs, the most famous of which were those of Waclaw Sierpinski in 1916, Karl Menger in 1926, and Paul Levy in 1937, were largely seen as trivial and unimportant until the publication of Benoit Mandelbrot's studies in 1975. He equated quantitative comparisons of simple fractals with real world observations. He also produced some striking pictures with then rudimentary computer display technology. Since his discoveries, fractals and chaos theory have become respected branches of mathematics whose modeling applications now range from population groups to the human nervous system.

A geometrical fractal is a figure composed of the same pattern, reduced and rotated infinitely many times. This defining property is called self-similarity, where the fractal's magnified sections are similar to the whole. Given only a picture of part of a fractal, it is usually impossible to tell what the scale of the picture is. This property is referred to as scale independence.

Fractals can be created by assigning a few arbitrary points and repeating an iterative rule over and over. The process is recursive and approaches completion as the number of iterations grows. Early on in his professional life, Sierpinski created an array of geometric fractals by choosing vertices of regular polygons and following an iterative rule to determine where to position the next point. After a sizeable number of points had been plotted, an (ideally infinitely) self-similar image had formed. The Sierpinksi pentagon is shown in Figure 1.

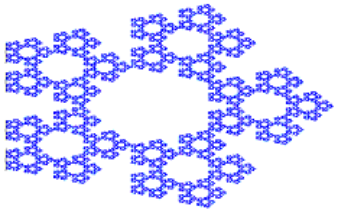

Figure 1: Sierpinski pentagon

The geometric fractals were called Sierpinski n-gons, each of which can be created by an algorithm that will be explained later.

Fractal shapes need not be restricted to regular polygons. In fact, by using specific and sometimes complicated iterative rules to plot new points, it is possible to create fractals that resemble real world shapes such as shorelines, seashell patterns, bronchial tubes and clouds. Fractals can also be used to draw textured landscapes such as lunar surfaces and mountains for use in advertisements and movies. Above all, fractals help to mathematically define the natural world.

Fractals also appear in a variety of physics problems. For example, the Henon map and Lozi map are two-dimensional fractal maps that describe astronomical orbits. The Navier-Stokes equations give rise to the Rössler attractor and the Lorenz attractor, both three-dimensional structures derived from fluid mechanics.

A necessary partner to fractals is chaos theory. The two are very much interconnected, and, unintuitively, there is an underlying chaos that can be used to create any fractal form. Chaos theory describes random data which are apparently disordered but actually have an underlying order. Behavior is difficult or impossible to predict and even very careful observation and measurements cannot give indications of how the system will act in the future. The theory was developed through Edward Lorenz's work during the 1960's in meteorology. His discoveries led to the famous butterfly effect, where he postulated that a single flap of a butterfly's wing can lead to a hurricane in another part of the world. A data set that is most commonly studied in chaos theory is a bifurcation graph (Figure 2). The graph starts with one line and begins to branch off in a rapid and chaotic fashion.

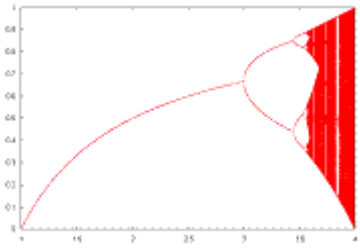

Figure 2: A sample bifurcation graph

Perhaps one of the most famous fractal sets is the Mandelbrot set. It is a set of complex numbers created via the iteration of a simple equation. Like any fractal, the Mandelbrot set is infinitely self-similar. The set is described by the amazingly simple recursive equation $z_{n+1} = z_n^2 + z_0$, which gives rise to a very intricate graph. The

Mandelbrot set is also related to the quadratic Julia sets in that each point in the Mandelbrot set corresponds to a different Julia set. Properties of these sets will be discussed later in detail.

The ultimate goal of this project was to use the knowledge obtained by exploring fractals to investigate a well known physical system, a ball bouncing on a vibrating plate. A perfect sphere bouncing on an oscillating plate was simulated and analyzed for fractal behavior. Fractal patterns of this ball were explored for various strengths of oscillations of the plate.

FRACTAL DIMENSION

Fractals are geometric shapes that have the characteristic of self similarity. The fractal dimension (more formally called the Hausdorff dimension) is the measure of a figure that corresponds to a mapping of an object between integer dimensions. Characteristics of a given fractal can be determined from knowing its fractal dimension. For instance, the values for fractals on a plane always fall between one and two. This shows that these fractals only "fill up" a portion of the plane, and are somewhere "between" a line and a plane (2).

The fractal dimension was calculated using the following two methods: the geometric formula and the box counting method. To use either of these methods the fractal must be considered as a set of points on a square grid. The grid is then divided into squares and the squares that contain any of the points in the set of the fractal are counted. The grid must be partitioned into squares that are self similar. This process is repeated five or six times using squares of different sizes (3).

With the box counting method, the values obtained from the previously explained process are employed to generate data, which is plotted in a double log plot. Plot the natural log of the number of squares containing the fractal versus the natural log of the inverse of the number of squares on one side of the grid. The slope of this line is the fractal dimension.

In the second method, the dimension is calculated according to the following equation:

$$\text{Dimension} = \ln(\text{self similar figures}) / \ln(\text{magnitude})$$

Using these two methods, the fractal dimension for the four following fractals were calculated: the Sierpinksi triangle, the fractal fern, the fractal maple tree, and the bifurcation map of the logistic equation.

Table 1: The Sierpinski triangle

Magnitude (n)	# of Squares (x)	Ln(1/n)	ln(x)	FD from slope	FD from formula
2	4	0.693147181	1.386294361	1.584962502	2
4	12	1.386294361	2.48490665	1.736965593	1.79248125
8	40	2.079441542	3.688879454	1.857980996	1.773976032
16	145	2.772588722	4.976733742	1.907553751	1.794977273
32	544	3.465735903	6.298949247	1.817492568	1.817492568

Table 2: The fractal fern

Magnitude (n)	# of Squares (x)	ln(1/n)	ln(x)	FD from slope	FD from formula
2	4	0.693147181	1.386294361	1.321928095	2
4	10	1.386294361	2.302585093	1.159171578	1.660964047
6	16	1.791759469	2.772588722	1.357552005	1.547411229
12	41	2.48490665	3.713572067	1.584962501	1.494451338
24	123	3.17805383	4.812184355	1.514192211	1.514192211

Table 3: The fractal tree

Magnitude (n)	# of Squares (x)	ln(1/n)	ln(x)	FD from slope	FD from formula
2	4	0.693147181	1.386294361	1.459431619	2
4	11	1.386294361	2.397895273	1.494764692	1.729715809
8	31	2.079441542	3.433987204	1.569404213	1.65139877
10	44	2.302585093	3.784189634	1.551795637	1.643452676
20	129	2.995732274	4.859812404	1.622245234	1.622245234

Table 4: The bifurcation graph of the logisitc function

Magnitude (n)	# of Squares (x)	ln(1/n)	ln(x)	FD from slope	FD from formula
8	38	2.079441542	3.63758616	1.574761559	1.749309171
10	54	2.302585093	3.988984047	1.773729554	1.73239376
13	86	2.564949357	4.454347296	1.260521513	1.736621927
15	103	2.708050201	4.634728988	1.842509619	1.711463468
20	175	2.995732274	5.164785974	1.724047913	1.724047913

Now, we will discuss how to create each of these fractals in more detail.

SIERPINSKI N-GONS

The career of the Polish mathematician Waclaw Sierpinski was one of the most profilic of the 20th century. In honor of his accomplishments, his name was bestowed upon

a fascinating set of geometric fractals. The main concept behind these fractals is to create fractals using basic geometric figures. The simplest example is the Sierpinski triangle. As the name implies, a triangle is the starting point for this figure. Although the one pictured is equilateral, this is not a requirement to generate the fractal. The triangle is split into four congruent triangles by connecting the midpoints of each side. The center triangle is then removed, and the process continues with the remaining triangles. The first three steps of this process are shown in Figure 3.

Figure 3: Steps 1-3 of constructing the Sierpinski triangle

Using a similar procedure, other Sierpinksi polygons can be generated. Although the triangle can be completely composed of similar triangles, most other polygons do not have this property of being self-tiled. Thus, for example, a Sierpinski pentagon (Figure 4) contains blank areas that do not resemble the original figure.

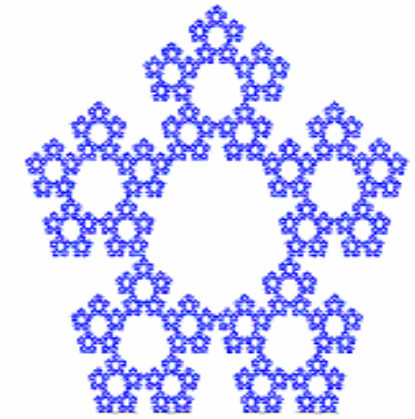

Figure 4: Sierpinski pentagon

There is another more interesting way to generate the Sierpinski fractals. First, start with a triangle and any point inside the triangle. Then randomly select one of the vertices of the triangle, and draw the midpoint between the vertex and the starting point. Now repeat, using this midpoint as the starting point. This eventually generates the Sierpinksi triangle as seen in Figure 5. This process can be generalized to more complicated figures. In this model, the vertices are called orbit points, because midpoints are being continually drawn towards them (5). We created a general formula for any n-gon, and used it to produce the famous Sierpinski 17-gon (Figure 6).

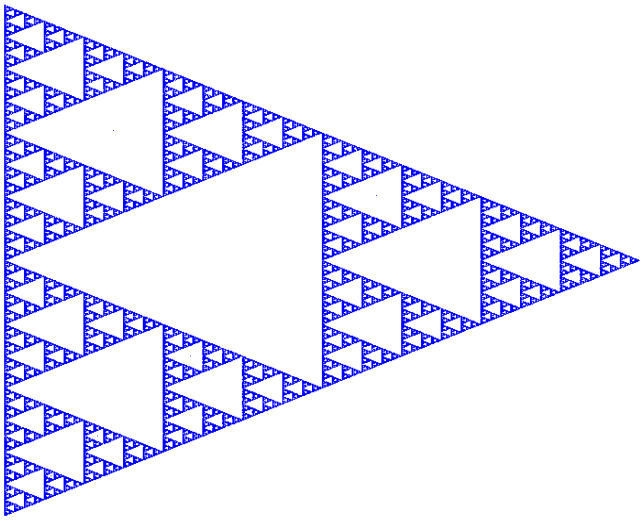

Figure 5: Sierpinski Triangle

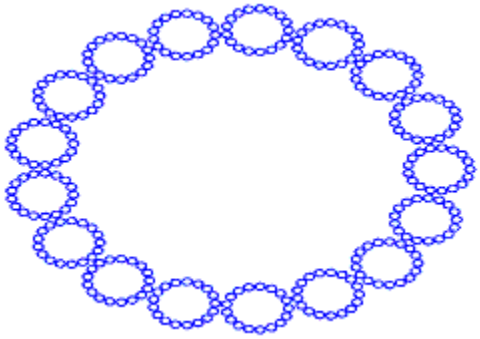

Figure 6: Sierpinski 17-gon

FRACTALS IN NATURE

Though fractals such as the Sierpinski triangle may seem to be purely mathematical phenomena, there are other properties of fractals that arise from a very different source - nature. Such fractals of the natural world often appear in the form of ferns, trees, clouds, pine cones, human bronchial tubes, and even bacterial colonies. Despite the variety of fractal behavior found in nature, they all contain the self-similar properties, scale independence, and infinite detail that defines them as true fractals (3).

Like fractals derived from formulaic calculation, fractals in nature are also capable of representation through algorithmic equations. Therefore, these fractal patterns can easily be created and displayed using a computer.

Fractal Fern

The fractal fern is created through a series of steps where points X_n, Y_n are inserted into their respective algorithms to produce X_{n+1} and Y_{n+1}. To construct the fractal fern's particular structure, various probabilities indicate exactly which formula to apply to X and to Y.

Table 5: Probabilities and formulae for fractal fern

Probability	X_{n+1}	Y_{n+1}
0.01	0	$0.16Y_n$
0.85	$0.85X_n + 0.04Y_n$	$-0.04X_n + 0.85Y_n + 1.6$
0.07	$0.20X_n - 0.26Y_n$	$0.23X_n + 0.24Y_n + 0.44$
0.07	$-0.15X_n + 0.28Y_n$	$0.26X_n + 0.24Y_n + 0.44$

Values for the initial X and Y are arbitrarily picked and new points are choosen through a large number of iterations of the equations in Table 5. The equation to use in each step is chosen using a random number generator and the probabilities stated in Table 5. Each resulting X and Y value is then plotted on a graph, and the image produced looks remarkably like a fern (Figure 7).

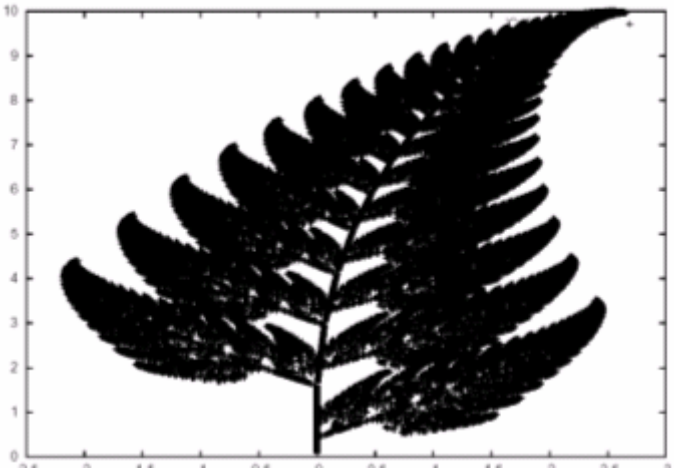

Figure 7: Fractal fern

Fractal Tree

Construction of the fractal tree follows the same procedure as that of the fractal fern. Variations only arise from the specific probability values and the algorithmic formulae, shown in Table 6 (5).

Table 6: Probabilities and formulae for fractal tree

Probability	X_{n+1}	Y_{n+1}
0.1	$0.05X_n$	$0.6Y_n$
0.1	$0.05X_n$	$-0.54Y_n + 1$
0.2	$0.46X_n - 0.32Y_n$	$0.39X_n + 0.38Y_n + 0.6$
0.2	$0.46X_n - 0.15Y_n$	$0.17X_n + 0.42Y_n + 1.1$
0.2	$-0.43X_n - 0.28Y_n$	$-0.25X_n + 0.45Y_n + 1$
0.2	$0.42X_n + 0.26Y_n$	$-0.35X_n + 0.31Y_n + 0.7$

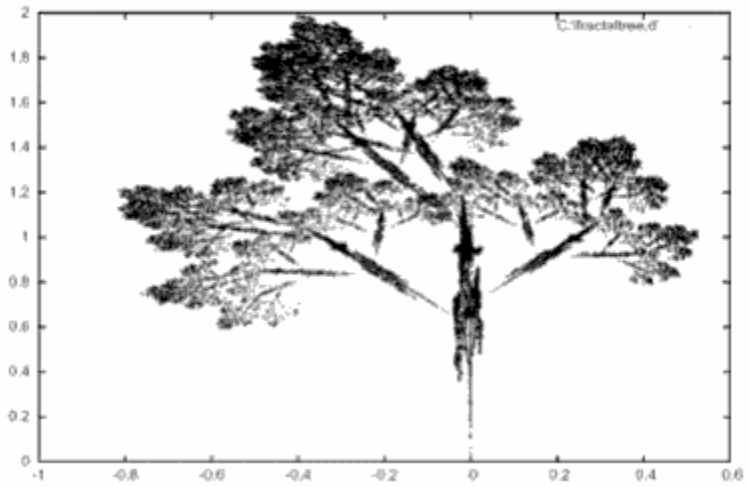

Figure 8: Fractal tree

FRACTALS IN PHYSICS

Certain physical systems and equations also produce fractals and chaotic structures. These include the Henon map, the Lozi map, and the Gingerbread man map. The first two are used in the study of astronomical orbits. All are 2-dimensional structures whose points are generated by recursive equations. For example, the equations for the Lozi map are:

$$x_{n+1} = 1 - a|x_n| + y_n$$
$$y_{n+1} = bx_n$$

Not all values of the coefficients a and b or initial point (x_0, y_0) produce the Lozi map. The values a = 1.7 and b = 0.5 and an initial point of (0, 0) were used to generate Figure 9. Similar procedures create the Henon map and Gingerbread man map (Appendix B).

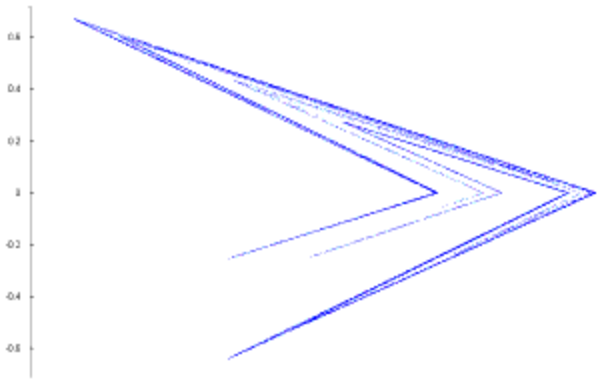

Figure 9: Lozi map

Also studied were the Rössler attractor and the Lorenz attractor, both of which are 3-dimensional structures derived from the Navier-Stokes equations for fluid dynamics. They are generated using differential equations. The Lorenz attractor, for example, can be produced using the following equations:

$$dx/dt = a(y - x)$$
$$dy/dt = bx - y - x$$
$$dz/dt = xy - cz$$

where x, y, and z are the coordinates of a point, and a = 10, b = 28, and c = 8/3. These equations are then discretized and iterated over as in prior examples. Again, the figure is dependent on the initial coordinates which were chosen to be (0, 3, 0) to create Figure 10. A similar procedure was used for the Rössler attractor (See Appendix B).

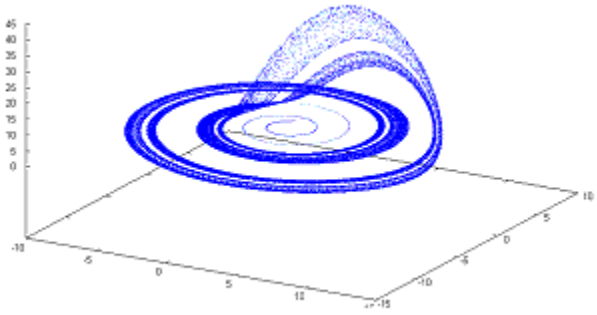

Figure 10: Rössler attractor

THE MANDELBROT SET AND JULIA SETS

A discussion of fractals would not be complete without discussing the Mandelbrot set (Figure 11). It illustrates the following three important properties of fractals: it can be generated by iterating a simple equation, it shows self-similarity, and it has both a finite

area and a fractal dimension. It is one of the most interesting fractals, aesthetically speaking, and has had much time devoted to it. The Mandelbrot set is defined by a deceptively simple equation,

$$z_{n+1} = z_n^2 + C.$$

The set consists of all values of C such that the z_n does not increase without bound as n goes to infinity. Any point z on the complex plane where $|z| > 2$ cannot be part of the Mandelbrot set (Appendix A for proof). The number of iterations it takes for z_n to exceed the $|z| = 2$ threshold is used to create the color coding of the Mandelbrot set. The Mandelbrot set itself is only the enclosed region displayed in black.

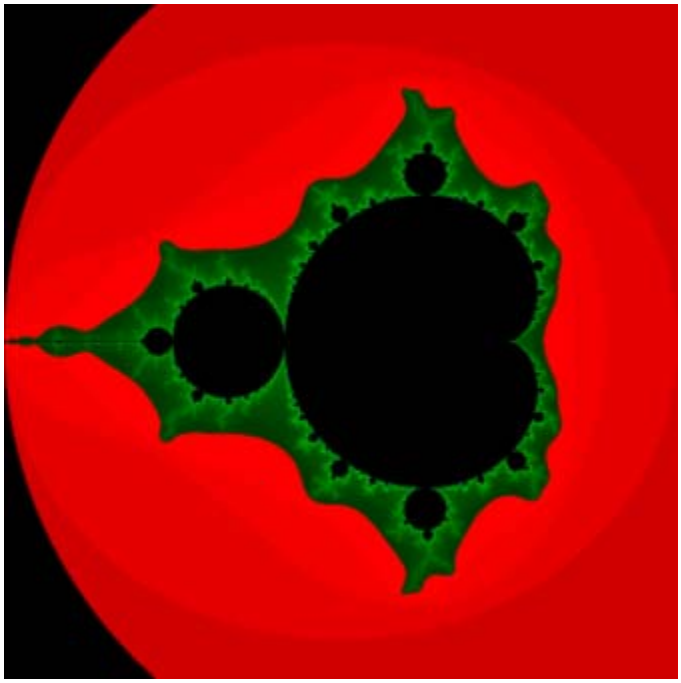

Figure 11: The Mandelbrot set

In generating the Mandelbrot set using a computer algorithm, we must consider both the number of iterations before convergence is accepted and the size of the region to display. Graphic representations of the fractal demonstrate the significance of the first factor. Looking at the rendition of the entire fractal, color transitions from shades of red to shades of green can easily be seen. Each of these colors represents a set of C's for which the z_n's exceeded 2 after a certain number of iterations. If 1 is used as the number of iterations before accepting convergence of a C, the circle r = 2 is produced rather than the Mandelbrot set. The more iterations used, the more the result looks like the Mandelbrot set. The portion of the plane displayed affects the number of iterations needed for a satisfactory image. If only a very small region near the border of the set is examined, more iterations would be needed than if the set were looked at as a whole.

Not only can the simple equation $z_{n+1} = z_n^2 + C$ map the Mandelbrot set, it can be used to map the quadratic Julia sets as well. The original purpose of the Mandelbrot set was

to describe the quadratic Julia sets. The Mandelbrot set itself represents the set of all points C such that the Julia set for each of those points is connected. The Julia set for C is mapped by iterating $z_{n+1} = z_n^2 + C$ for all different values of z_0 while holding C constant. These sets often appear similar to the region surrounding their corresponding point in the Mandelbrot set. Julia sets with C's in the large cardiod appear as one compact blob (Figure 12a). Border Julia sets resemble the border structures of the Mandelbrot set (Figure 12b). Julia sets with C's outside the Mandelbrot set are extremely fragmented sets referred to as Fatou or Cantor dust (Figure 12c). In this way, the Mandelbrot set and Julia sets can be used as tools to further explore one another (3).

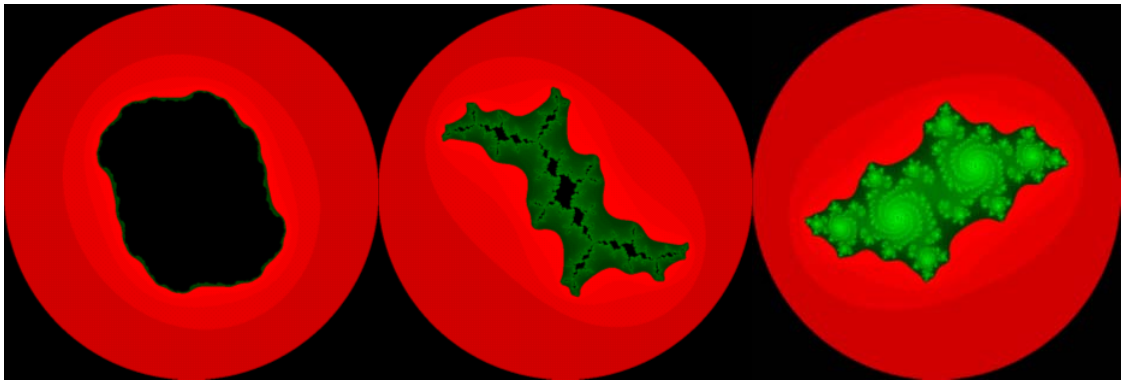

Figure 12: Three Julia sets

Self-Similarity and the Mandelbrot Set

The Mandelbrot set's self-similarity is evident from its graphic representation. The most noticable region of the set is the large cardiod on the right. Tangent to this cardiod at C = -.75 is a circle, and tangent to it at C = -1.25 is another circle. Zooming further in, more self-similarity becomes apparent. No matter how far you zoom in on the circular regions, it will still appear almost the same. An even more convincing example of self similarity can be found centered at C = -1.75. There can be found an almost identical replica of the Mandelbrot set. Self-similarity is plainly illustrated by zooming in around C = -1.26 - .475i (Figure 13). A spiral section of the Mandelbrot set looks under one magnification as if it were simply a rotated image of another.

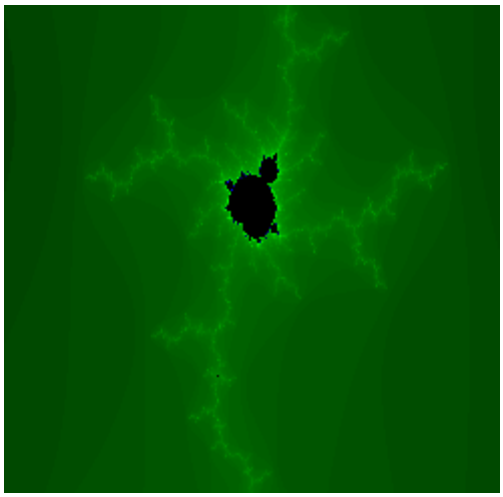

Figure 13: Mandelbrot set shown at coordinates [-1.276 + -.392i, -1.236 + -.364i]

Finite Area, Fractal Dimension, and the Mandelbrot Set

The Mandelbrot set is unbelievably intricate. So intricate, in fact, that the most powerful computers and the greatest mathematicians are able to give us only a range for the area covered by the set, and quite a wide one at that. The proof that it is finite is simple (because |z| must be less than 2, the circle r = 2 sets an upper bound for the possible area at 4π), but homing in on the exact number is far more challenging. There are many methods for approximating the area of the set, but most can agree on at least five digits after the decimal: 1.50659. When you consider that by the year 300, the Chinese mathematician Liu Hui approximated π to five digits, it is clear that there is much to learn about the Mandelbrot set.

It is known, however, that the border of the Mandelbrot set has infinite length, and that its fractal (Hausdorff) dimension is 2 (Mitsuhiro Shishikura published the proof of this in 1994). No fractal that can be mapped on the plane can have greater fractal dimension, for the plane itself has a dimension of 2. Thus, as far as fractal dimension goes, there exists no more complex planar fractal than the Mandelbrot set.

CHAOS THEORY

Chaos theory describes objects that appear disordered but actually have an underlying order. A bifurcation graph is an example of data that can be described by chaos theory. Bifucation is a process where a single solution to an equation splits and develops multiple solutions at specific points until the branching becomes so dense and indecipherable that the data can only be described by chaos. A bifurcation graph can be created using the logistic equation:

$$x_{n+1} = r * x_{n*} (1-x_n).$$

For low r, x_n converges to a single number. However, as r increases beyond 3, x_n will

oscillate between two values in a steady state. This process of splitting will continue, creating four values then eight then sixteen, and so on. The values of x_n will oscillate between the various values. Each splitting is referred to as a bifurcation. Beyond a certain critical value, the bifurcations stop and the value of x_n jumps around chaotically as shown in Figure 14.

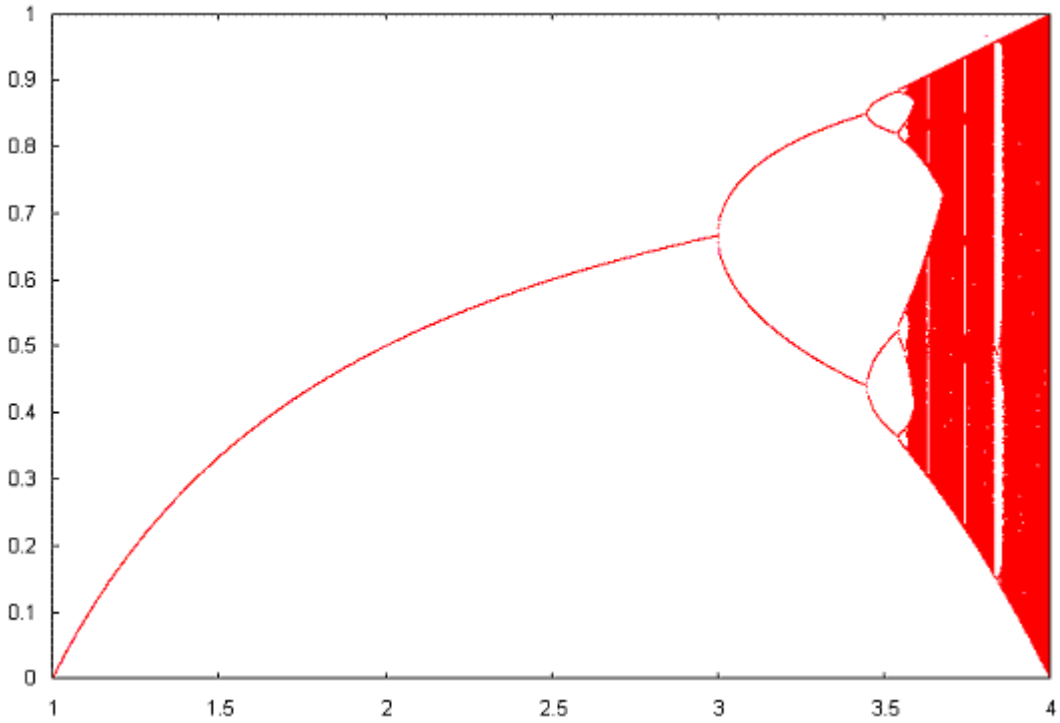

Figure 14: Bifurcation graph of the logistic function ($0 < r < 4$)

At $r = 4$ the x value drops down to 0 for an initial value of $x_n = 0.5$. After this point, the x values immediately drop to negative infinity and are no longer included in the bifurcation graph.

We then used the box counting method to determine the fractal dimension of this bifurcation graph. Since the box counting method specifies a square as the area that is in question, only the $3 < r < 4$ range of the bifurcation graph was analyzed. The fractal dimension of the bifurcation graph was found to be approximately 1.724.

The next challenge was to determine Feigenbaum's constant, δ. Feigenbaum's constant describes how quickly a function bifurcates and approaches chaotic behavior. It was discovered by Feigenbaum in 1975. As one can tell by looking at the bifurcation graph, the distance between each bifurcation becomes smaller and smaller. The constant is defined as the limit of $\Delta r_n/\Delta r_{n+1}$ as n goes to infinity where Δr is the change in r between succesive bifurcations. Table 7 gives an overview of the first few values in finding the constant.

Table 7: Calculation of δ

r	num. of branches	Δr	Δ
1.000	1		
3.000	2	2	
3.450	4	.45	4.444
3.544	8	.094	4.787
3.565	16	.021	4.476
3.570	32	.005	4.200

This process continues and δ approaches the value 4.669. This constant underlies the process of bifurcation, fractals, and chaos.

BALL IN OSCILLATING BED

Many real-world situations, such as the movement of shockwaves in an earthquake or sand blowing on a beach, can be simulated accurately by calculating each and every collision between particles. Considering the enormous number of particles involved in any realistic situation, this would take huge amounts of time on even the most powerful computers, and there are no obvious shortcuts. However, the overall result of each situation comes from many applications of fairly simple rules. This type of complexity arising from the repetition of simple calculations tends to show signs of fractal behavior. It may be possible to find fractal characteristics that describe the solution to these complex problems in terms of much simpler ones. Specifically, we simulated an ideal ball on a vertically vibrating plate.

This turned out to be a successful search for fractal behavior. Fractal behavior appears in the movement of the ball as the energy of the plate is increased. The quantity used to search for this fractal behavior is called Γ and is given by the equation

$$\Gamma = A\omega^2/g$$

where A is the amplitude of the plate's oscillation, ω is the frequency, and g is 9.8 m/s^2. As Γ is increased, one frequency was expected to be the only significant one. After a certain point, though, it was observed to split, and two frequencies were suddenly present. It was suspected that this splitting, or frequency bifurcation, would repeat many times at higher Γ, giving four, then eight frequencies. This could result in a bifurcation map which would show fractal behavior similar to the logistic map.

Creating a basic simulation was relatively simple. A program was created that expressed the ball and plate visually. The collisions were detected merely by testing whether or not the ball had passed below the top of the platform. If this event occurred, the ball would change direction, its new velocity would equal two times the velocity of the plate minus the velocity of the ball at collision. In addition to displaying the ball's motion, it produced data describing the ball's path and the frequency of its collisions. Graphing this

data provided clear evidence for bifurcation at lower values of Γ, creating four distinct collision paths with $\Gamma \approx 4.0$.

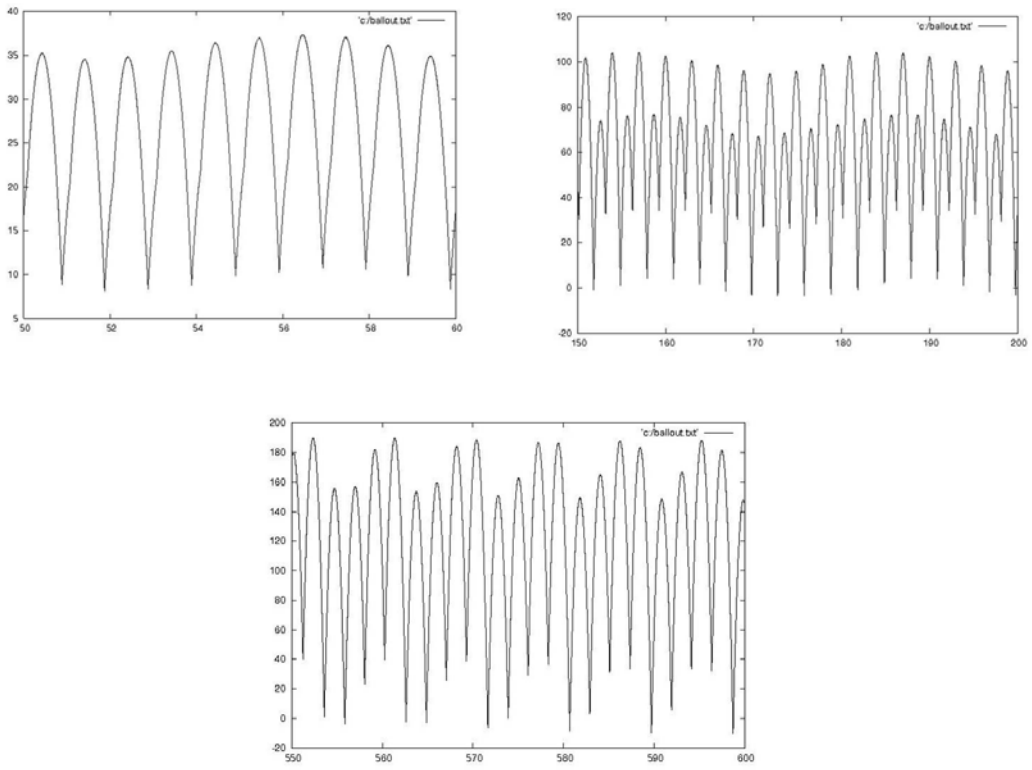

Figure 15: One frequency at $\Gamma \approx 1.67$, two frequencies at ~3, and four frequencies at ~4

In order to study the component frequencies, it was necessary to create a high-precision computer simulation. This was actually a much more complex problem than expected. The normal way to simulate such a system can have significant amounts of error, and the only way to reduce the error is to let the simulation use much greater amounts of computer time than was available. Instead, the simulation made use of a mathematical trick that allowed the possible collision range to be split into many pieces, each containing only one possible collision point, and then searched through each for the actual collision point. This allowed a much higher precision than would have been previously possible. Afterwards, a Fourier transform was used to split the results into the component frequencies.

After running the data through the Fourier transform[1], the result did not show any significant patterns in Γ, where bifurcation had already been clearly observed. Unfortunately, the Fourier transform was not capable of finding the splitting frequencies due to complex nature of the bifurcation. However, there is no dispute that the bifurcation itself does occur.

Stable and resonating phase constants and attractors

Perhaps the most notable observation made during the simulation process was that some values of Γ cause the system to approach a resonant frequency, that is a frequency that causes the ball to continuously gain energy reaching higher and higher heights. For resonant phase constants, the plate adds as much velocity as is needed to consume one or more extra periods of the plate's motion. In the simulation, the plate's frequency was held constant at 20 Hz. A little math and physics show the presence of stable and resonance points:

$$\Delta(\Delta t) = nT$$
$$2v/g = nT$$
$$v = ng/2f$$
$$\Delta v_{attack} = \pi ng/\omega = 2A\omega\cos(\varphi)$$
$$\pi n/2\Gamma = \cos(\varphi)$$

There is a trivial solution to the equation for any Γ, if $n = 0$ and $\varphi = \pi/2$ or $3\pi/2$. These two φ values represent the ridge and the trough of the plate's motion. If the ball is allowed to hit the plate at either of these phase shifts at any velocity of the form $ng/2f$, the ball will bounce off that same point ad infinitum. There are non-trivial solutions as well, but only for $\Gamma \geq \pi/2$. Only then can the plate generate enough speed to impart a large enough impulse on the ball so that it might jump ahead a period. Each φ where the plate velocity is positive has a corresponding φ equal to π-φ for which the plate velocity is negative (and thus the resonance is negative). Also, if φ is a resonance point, $-\varphi$ is also a resonance point. For $\varphi > \pi$, another quadruplet of resonance points appears.

The simulation, however, only discovered some of these resonance points. For several φ-values, the ball began oscillating around the resonances at almost the exactly the same time, and their final maximum heights were almost identical. In fact, all values of Γ between 3.147 and 3.311 reached maximum heights that were nearly identical. Never did the ball seem to oscillate around the resonances where $\sin(\varphi)$ was less than zero. The resonances were also clumped just after the values of $n\pi/2$.

The first observation may be somewhat of a fluke. The launch phase constant and velocity were very close to the phase constant and velocity of the resonance for those values of Γ, because those aspects of the launch were held dependent on Γ. The second and the third are more relevant, and are understood best in conjunction with one another. The phase constants that were a certain decimal greater than $\pi/2$ resulted in the ball converging around the resonance point, while those much greater than $\pi/2$ either took longer to converge or failed to converge at all.

It appears that some of the resonance points are acting as attractors, points that act much like the orbit points of the Sierpinski n-gons—which often cause fractal structure, as in the Lorenz and Rossler attractors. The attractors have the ability to correct φ-velocity pairs that are slightly off the resonant values. The most powerful attractors appear to be those with $\sin(\varphi)$ nearest zero. However, when $\sin(\varphi)$ gets very close to zero, the attractors

appear to lose their strength. A mathematical approach to the situation again provides the answer. When φ is just slightly less than the φ of resonance, the impulse the ball receives from the plate is stronger than it would receive at the φ of resonance. For example, it's just strong enough to kick it more than a period ahead for the next collision. The problem for attractors with very small φ is that their radius of attraction is very small. The attractor is effective only on φ values that are greater than –φ of resonance. It is only for those values which the velocity of the ball will be increased enough for it to skip more than a whole period of the plate's motion.

CONCLUSIONS

Many aspects of fractals were explored throughout the project. Combining the random walk method with the general magnification formula for Sierpinski n-gons, students created a program which generated the coordinates of any Sierpinski n-gon. Rather than relying on time-consuming and complex recursive processes, the Sierpinski n-gons were generated quickly using random numbers. Most of the other fractals were generated through simple iterative processes which proved to be sufficiently time-efficient. These fractals included naturally-occurring fractals, such as the fractal tree, the fractal fern, as well as fractals based on patterns in the complex number system, such as the Mandelbrot and Julia sets. Using either the box counting method or an equation based on the size and number of certain regular fractals, the fractal dimension of each of these patterns was determined, demonstrating that figures are not two-dimensional simply because they exist on a plane. Furthermore, these studies in fractals were applied to situations in classical physics, specifically in an attempt to assess the fractal nature of the frequency of a ball bouncing on a platform moving vertically via simple harmonic motion. A simulation of the ball's motion showed that as the frequency and amplitude of the platform were changed, the frequency of the ball's collisions bifurcated. Essentially, at still-undetermined values of Γ, a graph of frequency versus Γ would appear similar to the bifurcation graph of the logistic equation. Due to time constraints and the precision required for locating the fixed points, the graph could not be generated with the visual simulation.

The limited success of this simulation still provides sufficient leads to direct future experiments. One might write a purely mathematical analysis of the ball's movement and generate the data necessary for the creation of a bifurcation graph. In future studies, individuals might study the motion of several bouncing balls in two or even three-dimensional environments. Ultimately, the resulting studies in particle movement can be applied to real-world situations such as granular vibrations or earthquakes. Perhaps they can provide a more feasible means of simulating these complex environments. Concerning the other fractals, only a handful of patterns have been assessed in this study. Sierpinski's work can be applied to three-dimensional environments, generating fractals with yet-uncalculated fractal dimensions. Many more naturally-occurring fractals exist, including even many organs and organelles within the human body. These organic fractals have fractal dimensions between two and three, and thus can only be assessed in further studies of three-dimensional fractals. Mathematically, fractals can even be generated in environments with even four or more spatial dimensions. Students in this project were able

to implement the box counting method by drawing grids and counting squares. For future studies of higher-dimension fractals, mathematical and computer-dependent methods presumably must be implemented. It appears that each accomplishment in the field of fractals generates a number of questions exponentially greater than the number that it answers.

REFERENCES

[1] Eric W. Weinsteinn. "Lozi Map" From *MathWorld* -- A Wolfram Web Resource http://mathworld.wolfram.com/Lozimap.html
[2] Feder, Jens. Fractals. New York: Plenum P, 1988.
[3] Fractals in Science. Ed. Armin Bunde, and Shlomo Havlin. New York: Springer-Verlag, 1994.
[4] Paul Bourke. "The Rossler Attractor in 3D". Swinburne University of Technology in Melbourne, Australia. http://astronomy.swin.edu.au/~pbourke/fractals/rossler
[5] The Science of Fractal Images. Ed. Heinz-Otto Peitgen, and Dietmar Saupe. New York: Springer-Verlag, 1988.

APPENDIX A – DIVERGENCE OF POINTS OUTSIDE R = 2

Prove: $|z_k| > 2 \rightarrow \lim_{n\to\infty} z_n = \infty$

$when\ |C| > 2$

$|z_1| = |C^2 - C| \geq |C^2| - |C| > 2 = C$

$when\ |C| \leq 2$

$|z_k| > 2 \rightarrow |z_k| > |C|$

$|z_k^2| - |C| > 2|z_k| - |C|$

$|z_k^2 + C| > 2|z_k| - |C|$

$|z_{k+1}| > 2|z_k| - |C|$

$|z_{k+1}| - |z_k| > |z_k| - |C|$

$|z_{k+2}| - |z_{k+1}| > |z_{k+1}| - |C|$

$\Delta|z_{n+1}| > \Delta|z_n| > 0 : n \geq k$

$z_{k+s} \geq s\Delta|z_k|$

$\lim_{s\to\infty} s\Delta|z_k| = \infty$

$\lim_{s\to\infty} z_{k+s} = \infty$

QED

APPENDIX B – FRACTAL FORMULAE

Maple tree:

Probability	X_{n+1}	Y_{n+1}
0.10	$0.05X_n$	$0.6Y_n$
0.10	$0.05X_n$	$-0.054Y_n +1$
0.20	$0.46X_n-0.32Y_n$	$0.39X_n +0.384Y_n +0.6$
0.20	$0.47X_n-0.15Y_n$	$0.17X_n + 0.42Y_n + 1.1$
0.20	$-0.43X_n-0.28Y_n$	$-0.25X_n + 0.45Y_n + 1$
0.20	$0.42X_n + 0.26Y_n$	$-0.35X_n + 0.31Y_n + 0.7$

Fractal fern:

0.01	0	$0.16Y_n$
0.85	$0.85X_n + 0.04Y_n$	$-0.04X_n + 0.85Y_n + 1.6$
0.07	$0.02X_n – 0.26Y_n$	$0.23X_n + 0.22Y_n + 1.6$
0.07	$-0.15X_n + 0.28Y_n$	$0.26X_n + 0.24Y_n + 0.44$

Lozi:
$X_{n+1} = 1 – 1.7 |X_n| + Y_n$
$Y_{n+1}= 0.5 X_n$
Initial point (0,0)

Henon:
$X_{n+1} = 1 – 1.4X_n^2 * Y_n$
$Y_{n+1} = 0.3X_n$
Initial point (-1, 0)

Gingerbread
$X_{n+1} = 1 + |X_n| - Y_n$
$Y_{n+1} = X_n$
Initial point (-0.01, 0)

Rössler:
$dx/dt = -y – z$
$dy/dt = x + 0.2y$
$dz/dt = 0.2 + xz – 5.7z$
initial point (0, 1, 1) Δt : 0.04

Lorenz:
$dx/dt = 10(y – x)$
$dy/dt = 28x – y – xz$
$dz/dt = xy – 8/3z$
initial point (0, 3, 0) Δt : 0.02